

## A Two Dimensional Stress Analysis of Fixed Prosthesis with Rigid or Nonrigid Connectors

H. S. Yang, D. D. S., Ph. D.

*Associate Professor of Prosthodontics, College of Dentistry  
Chonnam National University, Kwang-Ju, Korea*

V. P. Thomposn, D. D. S., Ph. D.

*Professor of Fixed Prosthodontics, Dental School  
University of Maryland, Baltimore, MD 21201 USA*

A two dimensional finite element model was constructed to analyze the mechanical behavior of a five unit fixed partial denture(FPD) with a 2nd premolar pier abutment either employing a rigid or nonrigid connector. Gap elements were used to model the clearance space of the nonrigid connector. All FPDs with rigid or nonrigid connectors reduced the magnitude of stress in the periodontium as compared to the control, with both normal or reduced bone support. An FPD with rigid connectors induced the smallest stresses in the periodontium. A FPD with a nonrigid connector on the mesial of the molar abutment exhibited the most undesirable mechanical stress states and deformations.

### Introduction

The nonrigid connector is a broken-stress unit, and its design consist of key that is usually attached to the pontic and keyway which is placed in the retainer. Shillingburg and Fisher<sup>1)</sup> advocated a nonrigid connector at the distal surface of a pier abutment to prevent unfavorable leverage across the pier. Several authors<sup>2,3)</sup> suggested the nonrigid attachment as a solution for the mesially tilted molar abutment for a fixed partial denture.

Although the use of a nonrigid connector is widely considered in the case of a pier abutment or a tilted molar abutment, the nonrigid connector must be used discriminantly. The cantilever effect of the nonrigid design can induce an additional stress on an abutment and in time can destroy the supporting tissues. At present, there is insufficient scientific evidence to enable evaluation of the use of nonrigid connectors. Only a few photoelastic stu-

dies<sup>4,5)</sup> have been conducted concerning the stress analysis of a fixed partial denture with a nonrigid connector. Most of the information and indications for the use of nonrigid connectors were empirically derived.

The finite element method(FEM) of stress analysis is an useful and accurate tool to determine stresses and strains in a structure. Its validity in designing and analyzing prostheses has been established in dentistry<sup>6)</sup>. A two dimensional finite element method has been used to determine the stresses in a prosthesis and surrounding structures as well as the displacement of the abutment teeth caused by the forces of occlusion.

The purpose of this study was to qualitatively analyze the stress levels in the teeth and supporting structures and ascertain how addition of a fixed prosthesis with either a rigid or nonrigid connector modified these stresses and their distribution.

## Material and Methods

The finite element model was constructed of a mandibular posterior segment which included a canine, second premolar, second molar and supporting structures. A standard intraoral radiograph was made of a periodontally healthy mandibular premolar-molar area using the paralleling technique. There was no bone resorption and no abutment tilting. The radiograph was used to trace the outlines of each component and to construct the standard model (H, Fig. 1). The crown/root ratio of each tooth in this standard model was 1 : 1.5. Four variations of the two dimensional finite element model were constructed ; 1) no restoration, 2) a four unit fixed prosthesis with rigid connectors, 3) a four unit fixed partial denture with a nonrigid connector located on the distal of the 2nd premolar, and 4) a four unit fixed partial denture with a nonrigid connector located on the mesial of the 2nd molar. For each of the four models, another variation was made by reducing the alveolar bone level to a crown/root ratio of 1 : 0.6. The designs and their symbols are given in Table 1. The model included cortical and cancellous bone, dentin and enamel as well as the casting alloy where indicated.

In all models, the lower border of the mandible was modeled to be rigidly fixed in a vertical direction. The mesial border of the models was designed so that at the mesial contact point of the canine,

and at the upper and lower mesial border of the mandible the structure could deform elastically in a mesial direction with an assigned stiffness value of 20Kg/cm<sup>2</sup>. A 1Kg biting force with 15 degrees of mesial vector was applied on all of the fossae, marginal ridges of mesial vector was applied on all of the fossae, marginal ridges and cusps of the occlusal surface of each tooth (Fig 2). When a prosthesis was present loading of its fossae, and cusp tips was added to the total loading of the structures (Figs 14–16). The mechanical properties of the various materials were taken from the literature (Table 2). The elastic constant and Poisson's ratio of the materials, the data concerning coordinate and geometry of each node and element were input. The basic model (H) was comprised of 1214 2-dimensional elastic and 3 boundary elements and 1302 nodes, the spatial distribution of which varied with bone level and restoration.

The nonrigid connector was designed as a tapered key and keyway. A non-linear condition between key and keyway was possible by using 16 gap elements in modeling a nonrigid connector. This gap element was designed to not transmit compressive force until the clearance space between the key and keyway was completely closed. The connection between the elements in the interface was eliminated when tensile force occurred or when the structural deformation was insufficient to completely close the clearance space of the gap

Table 1. Symbols and designs of finite element models

Symbol	Design
H ;	No restoration, High bone level(C/R ratio of 1 : 1.5)
L ;	No restoration, Low bone level(C/R ratio of 1 : 0.6)
RH ;	Fixed partial denture with rigid connectors, High bone level.
RL ;	Fixed partial denture with rigid connectors, Low bone level.
PH ;	Nonrigid connector located distal of 2nd premolar, High bone level.
PL ;	Nonrigid connector located distal of 2nd premolar, Low bone level.
MH ;	Nonrigid connector located mesial of 2nd molar, High bone level.
ML ;	Nonrigid connector located mesial of 2nd molar, Low bone level.

Table 2. Mechanical properties of materials

Materials	Young's Modulus (Kg/cm <sup>2</sup> )	Poisson's Ratio
Enamel <sup>7)</sup>	$8.26 \times 10^5$	0.33
Dentin <sup>8)</sup>	$2.14 \times 10^5$	0.31
PDL <sup>6)</sup>	$7.03 \times 10$	0.45
Compact Bone <sup>9)</sup>	$1.45 \times 10^5$	0.30
Cancellous Bone <sup>10)</sup>	$2.15 \times 10^3$	0.30
Casting Gold <sup>6)</sup>	$8.46 \times 10^5$	0.40

element. Compression gap elements, which transmit force when the 0.08mm clearance space was closed, were installed on the vertical surfaces (axial wall) between the key and keyway. Zero clearance space compression gap elements were installed on the horizontal plane (pulpal wall) to allow immediate transmission of vertical compressive force (Fig. 3). The non-linear plane stress analysis program of Supersap Ver. 9.01/387 (Algor Inc. Pittsburgh, PA) was used to solve the problems.

The calculated numeric data were transformed into color graphics to better visualize the mechanical phenomenon occurring in the models. The maximum compressive stress, minimal tensile stress, and maximum shear stress in each model were calculated. By comparing these results, the effect of the fixed prosthesis with a nonrigid connector on the stress distributions and mobility of the supporting structures was evaluated.

### Results

As the stress level and distribution patterns of maximum compressive stresses are important in anticipating the breakdown of the peridontium by overloading, only plots of maximum compressive stresses are presented in this paper (Figs 4–11). In the periodontium, relatively high stresses were distributed in the cortical bone, but the size and value of the stress increased as the height of alveolar bone decreased (Figs 5, 6). All the FPDs modified and reduced the stress in the supporting struc-

ture. But high stress concentration area was observed around the rigid connectors of the structure near the nonrigid connector (Figs 9, 10). But high stress concentration area was observed under the connector area distal to the pier abutment and along the distal tooth surface of the premolar abutment (Fig. 11). For comparison of the magnitude of stresses in each model, the peak stress occurring in each material for each model was tabulated. The maximum compressive stresses of the free standing teeth in normal and reduced bone level group (H, L) were 106, 149Kg/cm<sup>2</sup> in the cortical bone and 10, 20kg/cm<sup>2</sup> in the PDL respectively. While the maximum compressive stresses of the FPD with rigid connectors in normal and reduced bone level group (RH, RL) were 93, 97kg/cm<sup>2</sup> in the bone and 7, 10kg/cm<sup>2</sup> in the PDL respectively. A FPD with a nonrigid connector on the mesial of the molar and reduced bone level (ML) showed the greater peak stress values in the PDL and bone than any other FPD group (Table 3).

In order to compare the mobility of an abutment teeth from model to model, the deflections were traced and shown in Figures 12–16. Note that the displacements were all magnified by a factor of ten for ease of visualization. In the un-restored groups, (H, L) the displacement of the teeth increased with the increasing bone resorption (Figs 12, 13). But the displacement of an abutment tooth decrease after insertion of a fixed prosthesis (Figs 14–16). The mesial and apical displacements in microns at the mesial cusp tip of the 2nd molar, the cusp

Table 3. Maximum stresses in the material of each design

		H	L	RH	RL	PH	PL	MH	ML
PDL	Comp. St.	10	20	7	10	8	11	9	12
	Tens. St	4	9	4	5	3	5	3	5
	Shear St.	5	10	4	5	4	6	4	6
Bone	Comp. St.	106	149	93	97	89	101	103	113
	Tens. St	101	128	73	65	64	58	102	118
	Shear St.	53	75	46	43	44	50	51	60
Tooth	Comp. St.	37	82	73	91	81	108	76	125
	Tens. St	20	57	40	61	37	47	66	98
	Shear St.	18	41	36	46	40	54	48	62
Gold	Comp. St.			371	395	424	475	261	354
	Tens. St			262	284	312	350	227	310
	Shear St.			185	197	212	238	131	177

Comp. st. ; Compressive stress, Tens. St. ; Tensile Stress.

(unit : Kg/cm<sup>2</sup>)

Table 4. Displacement of cusp tip in each design

Design	second molar		second premolar		canine	
	mesial	apical	mesial	apical	mesial	spical
H	139	68	109	27	88	19
L	287	142	300	47	133	26
RH	88	33	85	36	84	33
RL	94	38	92	44	91	45
PH	94	34	73	38	72	30
PL	106	39	79	47	78	42
MH	146	63	77	40	78	25
ML	169	76	79	50	81	35

(unit : microns)

tip of the second premolar and canine subjected to the standard loading conditions are listed. The displacement of free standing molar abutment with a normal and a reduced bone level (H, L) were 139, 287 microns in the mesial direction and 68, 142 microns in the apical direction respectively. But after insertion of a FPD with rigid connectors with a normal and a reduced bone support, (RH, RL) the displacement of a molar abutment decreased to 88, 94 microns in the mesial direction and 33, 38 microns in the apical direction. A FPD with a nonrigid connector on the mesial of the molar

showed the greater displacement of molar abutment than any other FPD at the same bone level (Table 4).

## Discussion

The nonrigid connector has long been advocated for use in restorative dentistry for prostheses dealing with a pier abutment, a tilted molar abutment or for multiple units. The female portion of the nonrigid connector is commonly placed within the normal tooth contours of the abutment. Although

this stress breaker configuration allows the individual tooth physiologic mobility, the cantilever effect of the nonrigid design can produce an additional, perhaps destructive stress to the abutment under the soldered retainer. Factors such as edentulous span length, occlusion, bone support and location of the nonrigid joint may affect the stress distribution around the abutment. If the compressive stress is excessive it can lead to alveolar bone resorption<sup>11)</sup>.

According to our calculations the greatest stresses in the periodontium of the un-restored teeth occurred around the root apex but relatively high stresses were also distributed in the cortical bone surrounding the root surface of the abutment teeth (Figs 5, 6). At a normal bone height (Fig 5), the maximum compressive stresses in the periodontal ligament (PDL) were 10Kg/cm<sup>2</sup>, while the magnitude of the peak stress with a reduced bone level was twice as large (Fig 6 and Table 3). When the level of the alveolar bone is normal, the periodontal surface area around the teeth become larger, the stresses are distributed into this larger area and the peak stress in PDL decreased.

The maximum compressive stresses for the fixed partial denture with rigid connectors and a low bone level were 10 and 97Kg/cm<sup>2</sup> in the PDL and bone respectively. These stress levels were similar magnitude to those calculated in the case of a high bone level and no restoration. When comparing the stresses between the unrestored group and the 5-unit fixed restoration, the magnitude of compressive stress in the PDL was reduced nearly 50% by the placement of a prosthesis in low bone level group (L, RL). In comparison a 20% reduction in stress was calculated when a prosthesis was placed on the teeth with normal bone levels (H, RH) (Table 3). The mechanical advantage created by a fixed prosthesis is more pronounced in situations with reduced bone support as compared to normal bone height as was determined in our previous work<sup>12)</sup>. When a FPD was present, the total occlusal force

increased because each cusp and fossa present (11 loading points with no restoration and 15 loading points with the 5 unit fixed prosthesis) was placed under the standard load. But deformation in the the prosthesis absorbed a major portion of the stress concentration in the prosthesis and reduces the overall stress level within the periodontium in comparison to the unrestored situation. Thus, the high elastic modulus of the metal reduced the overall stress level within the periodontium (Figs 5-8). This result complements other stress analysis research on fixed prostheses<sup>6, 13)</sup> and indicates a possible periodontal advantage of high modulus base metal alloys as opposed to gold alloys. As anticipated based upon the above results, the mesial and apical displacement of the abutment teeth increased with bone resorption (Fig. 12) and decreased after insertion of a fixed prosthesis (Figs 13, 14).

In case of the FPDs with the nonrigid connector the peak stresses in the periodontium, at the same bone height, are not very different when compared to the FPD with rigid connectors. Some authors<sup>1)</sup> claim that the pier abutment in the fixed restoration acts as a fulcrum and will generate considerably higher stresses around the pier abutment. But the results of our study are to the contrary and indicate no excess stress was generated in the periodontium around the pier abutment when restored with a fixed partial denture (Figs 7-8). Because of the excellent absorption and distribution of the occlusal stresses into the fixed prosthesis, the fulcrum phenomenon was not observed around the pier abutment in the FPD with rigid connectors. The highest value of stress was produced in the metal around the region of the rigid connectors, while relatively low stress levels were found in the region of the nonrigid connector (Figs 9-11). Although a high stress concentration was found in the metal structure of the rigid connector, a fixed prosthesis reduced the stress level in the supporting periodontal structures in all situations.

The effect of nonrigid connector location was also examined in this study. The peak compressive stress in the PDL around the molar was  $4\text{Kg}/\text{cm}^2$  with both the rigid connector (RH) or the non-rigid connector located on the distal of the second premolar (PH), while moving the non-rigid connector to the mesial of this pier abutment (MH) resulted in an increase to  $9\text{Kg}/\text{cm}^2$ . The peak compressive stress in the bone around the pier abutment was  $59\text{Kg}/\text{cm}^2$  for both RH and PH and  $70\text{Kg}/\text{cm}^2$  for MH. Additional high stress concentration occurred under the connector along the distal surface of pier abutment when a nonrigid connector was placed on the mesial of the second molar abutment in both MH and ML (Fig. 11). The cantilever action of nonrigid connector in MH and ML may be the cause of high stress concentration at this area. At a given level of bone support, the the ML and MH models generated higher compressive stresses in the periodontium than any of the other FPD models (Table 3). The FPD with rigid connectors and the FPD with a nonrigid connector at the distal of the pier abutment resulted in the smallest peak stresses in the periodontium and demonstrated similar stress distribution patterns (Figs 7, 9).

At the same bone level a FPD with a nonrigid connector on the molar (ML) exhibited a greater abutment mobility than a FPD with the nonrigid connector on the premolar (PL Figs 15–16 Table 4). The placement of the nonrigid connector at the mesial of the molar with the reduced bone level (ML) resulted in the highest peak stress in the periodontium and the greatest mobility of the molar abutment. A photoelastic study 4 has also shown that placement of a nonrigid connector at the mesial of the distal abutment is least desirable. A likely reason for the difference in stress levels in FPDs between the locations of the nonrigid connectors was the mesial component of the occlusal force vectors. If the keyway of the connector is placed on the distal side of the abutment, mesial movement seats the key into the keyway more solidly, while

the placement of the keyway on the mesial side allows no buttressing effect until larger displacements occur.

Although two dimensional finite element analysis of dental structures were not an exact representation of the real situation, the results obtained have significant clinical implications. The better distribution of the occlusal force was achieved with a fixed prosthesis with rigid connector as compared to the free standing teeth or any other FPDs with a nonrigid connector. The nonrigid designs resulted in a greater or equivalent value of peak stress in the periodontium when compared to the rigid FPD. No stress concentration was observed around the pier abutment after placement of a FPD with rigid connectors. But the placement of a nonrigid keyway at the distal of the abutment was the preferable place of nonrigid connector. Even with the optimal placement of a nonrigid connector, it is unlikely that the use of nonrigid connector reduce the excess stresses of the periodontium. Based upon this stress analysis a clinical problem associated with a fixed restoration with a nonrigid connector is fatigue failure at the rigid connector because of the higher stress levels in this area with such designs.

It is evident that a three dimensional model and more accurate material properties, particularly with regard to modeling the periodontium, would yield more accurate stress values and distributions. Further FEM studies using a 3-D model and long-term clinical data are needed to confirm the generality of the above results.

## Conclusions

Within the limitations imposed by a two dimensional finite element analysis the following conclusions can be drawn:

1. In the un-restored model with a reduced bone level, the highest peak stresses were generated in the periodontium and the greatest tooth mobility was observed.

2. All fixed restorations, whether with rigid or nonrigid connectors, reduced the stress in the periodontium by absorption and distribution of stresses by deformation within the prosthesis, and showed smaller cuspal displacement than the un-restored models.

3. The mechanical advantage gained by a FPD is more pronounced in situations of reduced bone as compared to normal bone support.

4. A FPD with rigid connectors induced the smallest peak compressive stress in the periodontium.

5. A FPD with a nonrigid connector on the mesial of the molar exhibited the most undesirable mechanical behavior.

## REFERENCES

1. Shillingburg HT, and Fisher DW : Nonrigid connectors for fixed partial dentures. *J Am Dent Assoc* 1973 ; 87 : 1195–1199.
2. Rosenstiel SF, Land MF, and Fujimoto J : Contemporary fixed Prosthodontics. 1st ed. St. Louis, C. V. Mosby Co., 1988, pp. 46–47.
3. Malone WFP, and Koth DL : Tylman's theory and practice of fixed prosthodontics. 8th ed. St. Louis, IEA Inc, 1989, pp. 16–18.
4. Moulding MB, Holland GA, and Sulik WD : Photoelastic stress analysis of supporting alveolar bone as modified by nonrigid connector. *J Prosthet Dent* 1988 ; 59 : 263–274.
5. Sutherland JK, Holland GA, Sluder TB, and White JT : A photoelastic analysis of the stress distribution in bone supporting fixed partial dentures of rigid and nonrigid design. *J Prosthet Dent* 1980 ; 44 : 616–623.
6. Farah JW, Craig RG, and Meroueh KA : Finite element analysis of three-and four-unit bridges. *J Oral Rehab* 1989 ; 16 : 603–611.
7. Craig RG, Peyton FA, and Johnson DW : Compressive properties of enamel, dental cements, and gold. *J Dent Res* 1961 ; 40 : 936–945.
8. Grenoble DE, Katz JL, Dunn KL, Gilmore RS, and Murty KL : The elastic properties of hard tissues and apatites. *J Biomed Mater Res* 1972 ; 6 : 221–233.
9. Carter DR, and Spengler DM : Mechanical properties and composition of cortical bone. *Clin Orthop Rel Res* 1978 ; 135 : 192–217.
10. Carter DR, and Hayes WC : The compressive behavior of bone as a two-phase porous structure. *J Bone Jnt Surg* 1977 ; 59A : 954–962.
11. Reitan K : Clinical and histological observations on tooth movement during and after orthodontic treatment. *Am J Orthod* 1967 ; 53 : 721–745.
12. Yang HS, and Thompson VP : A two dimensional stress analysis comparing fixed prosthetic approaches to the tilted molar abutment. *Int J Prosthodont* 1991 ; 4 : 416–424.
13. Glickman I, Roeber FW, Brion M, and Pameijer JHN : Photoelastic analysis of internal stress in periodontium created by occlusal forces. *J Pe-*

## Legend

- Fig. 1. Color code for the material present ; cancellous bone(green), compact bone(red), PDL (yellow), dentin(blue) and enamel(brown)
- Fig. 2. Two-dimensional finite element model at high bone level. Arrows indicate applied load. Triangle marked nodes are fixed in X and Y direction. Nodes with a circle are fixed in X direction.
- Fig. 3. Design of the nonrigid connector. Pink and blue colors represent gold alloy and dentin respectively. Six compressive gap elements with 0 gap space are installed vertically between gingival wall of the key and keyway. Ten compressive gap elements with 0.08mm clearance are installed horizontally between the axial walls of the key and keyway.
- Fig. 4. Compressive stress magnitudes and associated color for figures 5–11. Unit : Kg/cm<sup>2</sup>.
- Fig. 5. Stress distribution with no restoration and ideal bone height(H). Stresses are distributed around the root apex and more widely in the cortical bone.
- Fig. 6. Stress distribution with no restoration and low bone level(L). Higher and wider stress concentrations are observed in the periodontium around the root apices as compared to the normal bone height in Fig. 5.
- Fig. 7. Stress distribution with high bone level and 5-unit restoration(RH). The FPD not only reduces the stress level but also modifies the pattern of stress distribution. Stress is relieved in the periodontium. High stress concentrations are seen in the connectors of the fixed prosthesis.
- Fig. 8. Stress distribution with low bone level and FPD(RL). The prosthesis markedly reduced the stress in the periodontium when compared to Figure 6. No localized stress concentration is found in the periodontium around the pier abutment after installation of the FPD.
- Fig. 9. Stress distribution with ideal bone height and FPD with nonrigid connector at the distal of the pier abutment(PH). Similar pattern of stress distribution to FPD with rigid connector(Fig. 7) is observed.
- Fig. 10. Stress distribution around the nonrigid connector in PH. Compressive forces are transferred to the keyway by the vertically directed gap element. The high stress area around the connector is not so wide.
- Fig. 11. Stress distribution with high bone level and FPD with nonrigid connector on the mesial of the second molar abutment(MH). When compared to Figure 9 additional compressive stress is generated in the periodontium on mesial surface of the mesial root of the molar abutment and on the distal root surface of premolar. High stress in the prosthesis is found around the rigid connector at the distal of the pier abutment.
- Fig. 12. Deflection of the dental structures with a high bone level(H). Green lines indicate the outline before loading. White lines show the contour after loading. Magnitude of displacement X 10.



- Fig. 13. Deflection of the dental structures with a low bone level without restoration(L). Increased mobility of the abutment teeth is observed. Magnitude of displacement X10.
- Fig. 14. Deflection after the insertion of a FPD with rigid connectors and reduced bone level (RL). A marked reduction in the abutment mobility is seen. Magnitude of the displacement X 10.
- Fig. 15. Deflection with reduced bone level and a FPD with a nonrigid connector to the distal of the premolar(PL). Magnitude of the displacement X 10.
- Fig. 16. Deflection after the insertion of a FPD in the presence of reduced bone support with a nonrigid connector to the mesial of the molar abutment(ML). Magnitude of the displacement X 10.

## 비고정성 연결장치를 갖는 가공의치의 응력분석

전남대학교 치과대학\*

메릴랜드 대학교 치과대학

양홍서\* · Van P. Thompson

제 2소구치를 중간지대치로 하고 고정성 및 비고정성 연결장치를 갖는 5unit 가공의치에 의해 발생하는 역학 현상을 규명하기 위하여 이차원 유한요소 모형을 제작하였다. 비고정성 연결장치의 간극을 부여하기 위하여 gap element를 사용하였다. 연결장치의 종류나 치조골의 흡수 정도에 상관없이 모든 가공의치는 치근막 내에 발생하는 응력을 감소시키는 역할을 하였다. 그중에서 고정성 연결장치를 갖는 가공의치에서 치근막 내에 가장 작은 응력이 발생하였다. 대구치의 근심면에 비고정성 연결장치를 갖는 가공의치가 역학적 응력과 변위의 관점에서 바람직하지 않았다.

사진부도①

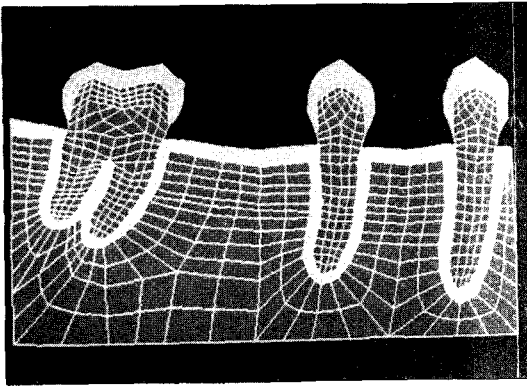


Fig. 1.

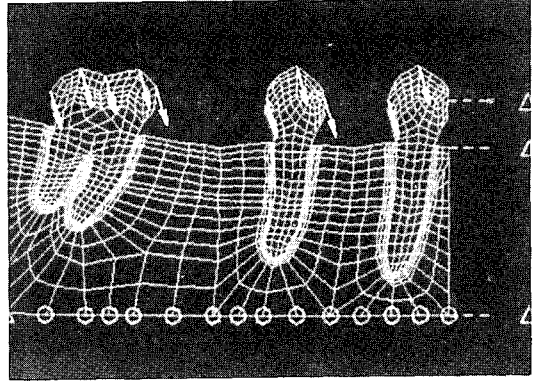


Fig. 2.

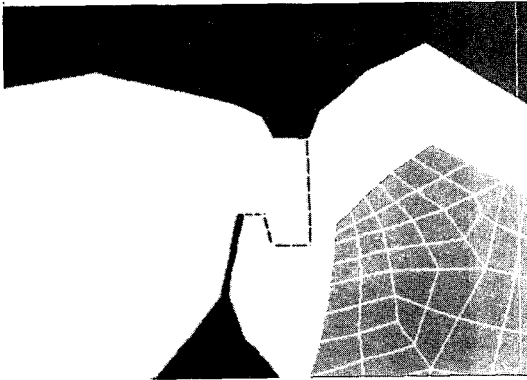


Fig. 3.

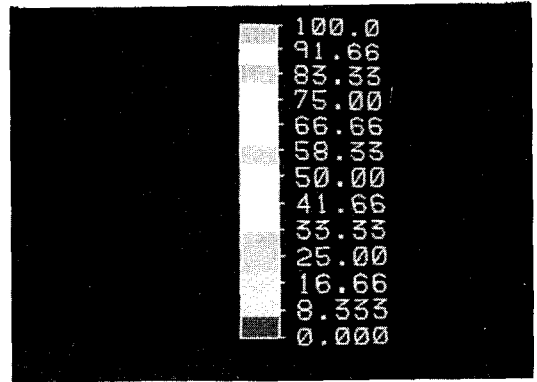


Fig. 4.

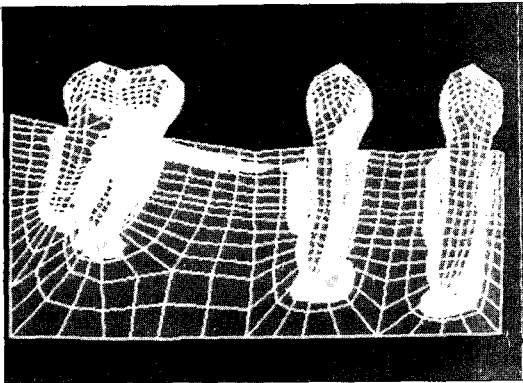


Fig. 5.

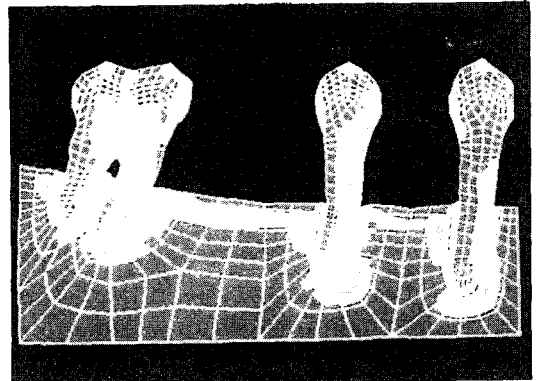


Fig. 6.

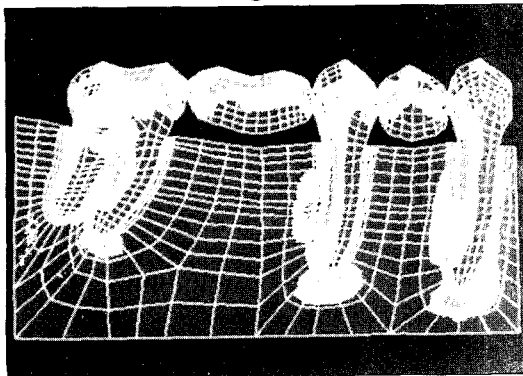


Fig. 7.

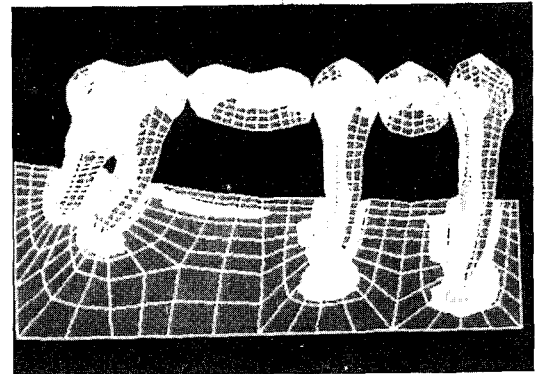


Fig. 8.

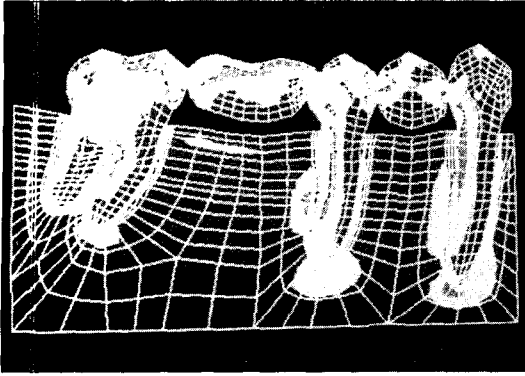


Fig. 9.

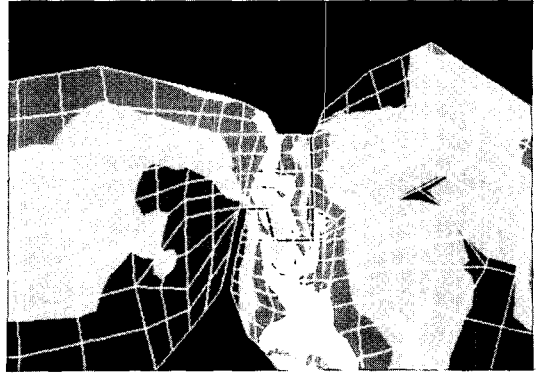


Fig. 10.

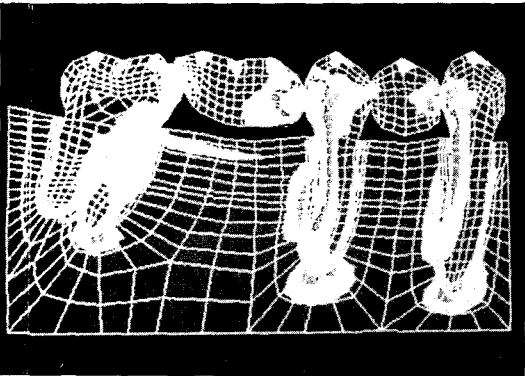


Fig. 11.

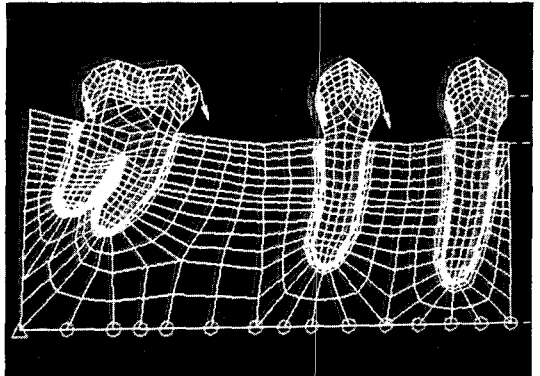


Fig. 12.

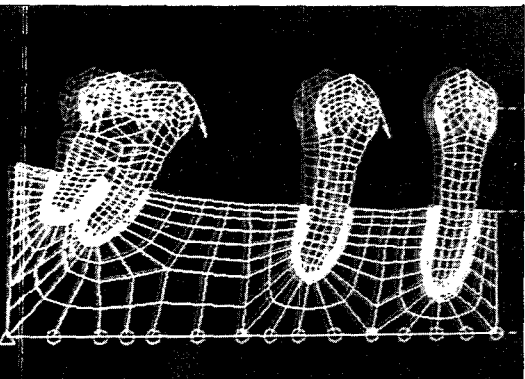


Fig. 13.

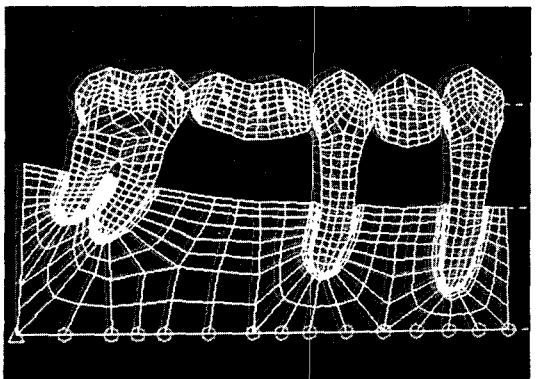


Fig. 14.

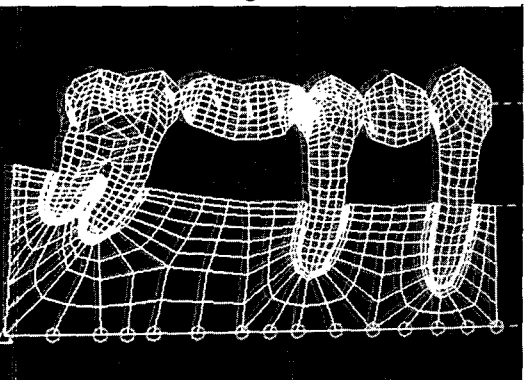


Fig. 15.

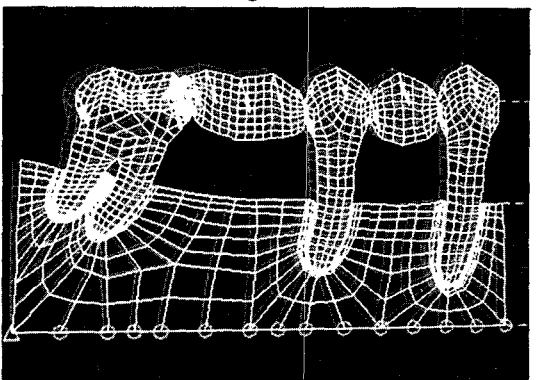


Fig. 16.